Use of Weather Radar for Flood Forecasting in the Sieve River Basin: A Sensitivity Analysis

MARCOS L. PESSOA, RAFAEL L. BRAS, AND EARLE R. WILLIAMS

Massachusetts Institute of Technology, Cambridge, Massachusetts

(Manuscript received 18 September 1991, in final form 22 August 1992)

ABSTRACT

Weather radar, in combination with a distributed rainfall–runoff model, promises to significantly improve real-time flood forecasting. This paper investigates the value of radar-derived precipitation in forecasting streamflow in the Sieve River basin, near Florence, Italy. The basin is modeled with a distributed rainfall–runoff model that exploits topographic information available from digital elevation maps. The sensitivity of the flood forecast to various properties of the radar-derived rainfall is studied. It is found that use of the proper radar reflectivity–rainfall intensity (Z–R) relationship is the most crucial factor in obtaining correct flood hydrographs. Errors resulting from spatially averaging radar rainfall are acceptable, but the use of discrete point information (i.e., raingage) can lead to serious problems. Reducing the resolution of the 5-min radar signal by temporally averaging over 15 and 30 min does not lead to major errors. Using 3-bit radar data (rather than the usual 8-bit data) to represent intensities results in significant operational savings without serious problems in hydrograph accuracy.

1. Introduction

Meteorological radar has long been recognized for its ability to provide estimates of precipitation at high spatial and temporal resolution. The increased access to digitized radar-derived precipitation and the availability of geographical information systems, particularly digital elevation maps, have motivated the development of a new generation of distributed rainfall–runoff models. These models operate on grid-based, high-resolution descriptions of river basins. They trade lumped parameterizations for the newly found wealth of spatially distributed data. Potentially, they will provide better and more timely real-time flood forecasts anywhere in the modeled river basin.

The objective of this paper is to study how sensitive the streamflow prediction is from one of the aforementioned models to characteristics of the radar-derived precipitation.

A distributed basin simulation model (DBS) is used. The model was developed at the Massachusetts Institute of Technology's (MIT) Ralph M. Parsons Laboratory (Cabral et al. 1990; Garrote 1992) with the intent of integrating detailed topographical information from digital elevation maps with a physically based, but efficient, formulation of the runoff production process in its grid-based structure. The model is calibrated to the Sieve Basin (840 km^2), near Florence, Italy (Cabral et al. 1990).

Corresponding author address: Dr. Rafael L. Bras, Department of Civil and Environmental Engineering, Massachusetts Institute of Technology, Cambridge, MA 02139.

Two sets of radar-derived precipitation are used to obtain the discharge predictions. One is a set of "deep convective" storms from Darwin, Australia. They consisted of short-lived moderate intensity cells. These storms were recorded by the MIT C-band radar. The other set consists of stratiform, more spatially uniform, storms from New England, recorded by the MIT S-band radar. The strategy is to manipulate the radar data to create precipitation inputs with a variety of resolutions in time and space. The streamflow response to this variety of inputs is then studied. Naturally, we are creating an artificial experiment, limited by the rainfall, the Sieve Basin properties, and the rainfall–runoff model used. Nevertheless, it is believed that results may be representative of more general situations.

After a brief description of the distributed flood forecasting model, the paper will present results:

1) the impact of precipitation time resolution on the predicted hydrograph,
2) the impact of precipitation spatial resolution on the predicted hydrograph,
3) the impact of the numerical accuracy of precipitation data, and
4) the impact of a variety of reflectivity–rainfall calibrations.

As stated, the objectives of this work are fairly focused. It is not intended to cover all aspects of radar meteorology, rainfall–runoff modeling, and forecasting. These are extensive subjects with innumerable related publications. For a good review of radar and other precipitation remote-sensing techniques, the reader is re-

© 1993 American Meteorological Society

Unauthenticated | Downloaded 04/18/24 09:57 AM UTC

ferred to Browning and Collier (1989) or Collier (1989). Meteorological radar and some of its difficulties are also discussed by Krajewski (1987) and Smith and Krajewski (1987). Georgakakos and Kavvas (1987) review and provide a large number of references addressing radar use for precipitation analysis, modeling, and prediction for hydrologic purposes.

Goodrich and Woolhiser (1991) review the recent history of catchment hydrology. Georgakakos (1986) outlines the coupling of rainfall and streamflow forecasting in a real-time mode using a lumped streamflow prediction model. Hudlow (1988) discusses United States practice in real-time operational hydrologic forecasting. Georgakakos and Smith (1990) discuss results of a real-time flood forecasting experiment using conceptual hydrologic models developed for the U.S. National Weather Service.

2. The DBS rainfall–runoff model

DBS is a distributed, physically based, flood-forecasting model that was developed by Cabral et al. (1990) and Garrote (1992). The model uses the grid of a digital elevation map (DEM) as spatially discrete elements, each one consisting of a spatially homogeneous soil column described by its geometrical and pedological characteristics. The discrete spatial representation allows for the distributed definition of terrain slope, soil parameters, and rainfall input.

DBS accounts for two types of runoff generation processes: 1) Hortonian and 2) saturation from below. The kinematic approximation is used to simulate the movement of water under the soil surface in both saturated and unsaturated flows. The flux of subsurface water is governed by Darcy's equation. The Brooks–Corey parameterization scheme (Brooks and Corey 1964) is adopted to relate the unsaturated hydraulic conductivity and the pore pressure with water content. The saturated hydraulic conductivity is assumed to decrease exponentially with depth.

Under the kinematic approximation, the infiltration capacity of a soil column is then equal to the saturated hydraulic conductivity at the surface. A rainfall intensity I at the surface, higher than the saturated hydraulic conductivity K_{sat}, would produce a Hortonian infiltration–excess runoff equal to $I - K_{sat}$. Additional water moves into the soil, and the model calculates a soil moisture distribution and its movement in time. The heterogeneity in the vertical distribution of hydraulic conductivity may lead to the formation of a zone of perched saturation. The bottom saturated front moves down and propagates at a rate controlled by the heterogeneous soil properties. If the infiltrating water exceeds that rate, the top boundary of the perched saturation zone ascends as the storm progresses, and it may eventually reach the surface producing a "saturation from below" type of runoff generation. The model fully accounts for the evolution of the zone of perched saturation, which is bounded by two sharp discontinuities in the moisture profile: 1) the wetting front depth (moving down), and 2) the top front depth (which may move up or down).

Local terrain slope, heterogeneity, and anisotropy in the soils lead to nonvertical infiltration in the unsaturated and saturated zones of the soil column. Therefore, lateral movement of water may exist. The model accounts for this transfer of water between elements through mass-conservation arguments. Whenever the sum of the total water content M_t in the element and the net lateral flow exceeds the capacity of the unsaturated soil zone above the wetting front to hold water, return flow is generated. This return flow is added to the surface runoff volume.

The detailed geomorphological description provided by DEMs allows the routing of runoff using the simple concept of travel time. Algorithms for extracting the river channel network from a DEM are used to identify the path that runoff generated at the surface of a soil column (pixel) would follow down to the basin outlet (Tarboton et al. 1989). The travel time is defined by parameterizing overland and streamflow velocities as a function of outlet discharge or as constants. Overland flow is assumed to be a quickly "channelized" process, and therefore, the model does not account for infiltration of surface runoff during the routing process.

A constant-flow-velocity assumption allows for a linear approach to the computation of the hydrograph at the outlet of the basin. An incremental basin response can be estimated independently for every time step. The computations are performed following a discrete time loop in which surface runoff generation and moisture balance within and between pixels are computed. Resulting surface runoff is then routed to the basin outlet.

Three state variables (the moisture content, the wetting front depth, and the top front depth) define the moisture state in every pixel. Below the wetting front the water profile is the one corresponding to the initial state before the beginning of the storm. Between the wetting and the top fronts the soil column is saturated. The wetting and the top fronts coincide if the moisture profile has not reached saturation anywhere. The evolution of the state variables is described by a number of first-order differential equations (see Cabral et al. 1990; Garrote 1992), and a finite-difference scheme is used to compute the evolution of the state variables for every time step.

The incremental response computed by the model at every time step is a function of the initial state (described by the state variables) and the input data (distributed rainfall). The model is computationally efficient in real-time applications: A description of the final state in the last run of the model can be used as initial state in the next calculation step, and the model

Unauthenticated | Downloaded 04/18/24 09:57 AM UTC

can be run incrementally as new rainfall data becomes available.

Figure 1 offers a simplified schematic representation of the DBS model, showing the main datasets that are used. The geomorphologic datasets are the soil types (different hydraulic properties are attributed to each soil type), the slopes, the direction of the outflow from each pixel, the distances to the nearest stream, and the distances to the outlet of the basin (sum of the distance to the nearest stream and the distance from there to the outlet along the stream). The initial state of the basin is described in terms of surface and subsurface moisture conditions, which are summarized by the water-table depth; the total moisture content; the wetting front depth; and the top front depth.

All these datasets can be obtained either in real time as the output from other hydrological modeling, such as long-range water-balance models (Becchi et al.

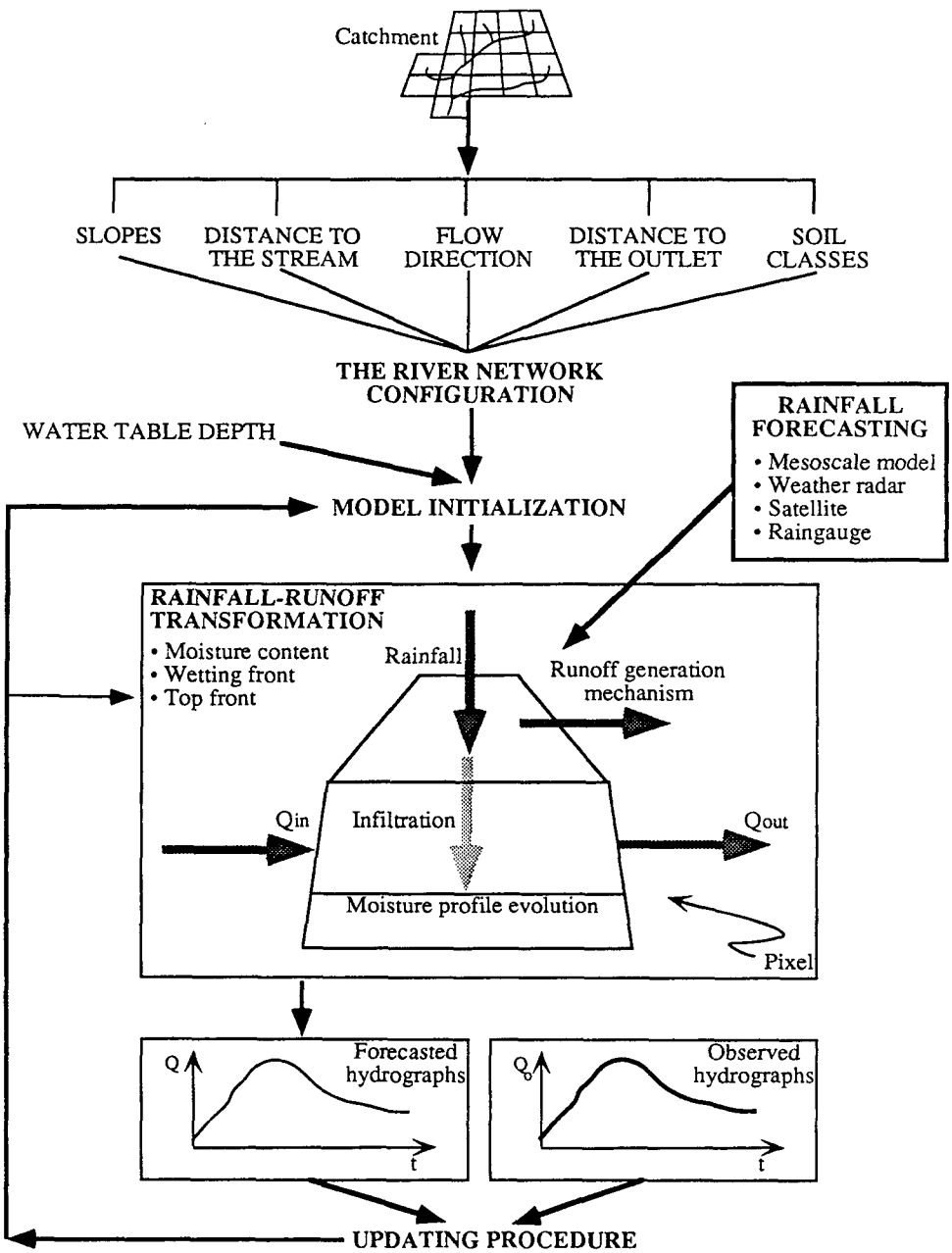

FIG. 1. A schematic representation of the DBS rainfall–runoff model data.

Unauthenticated | Downloaded 04/18/24 09:57 AM UTC

1989), or by the interpretation of satellite imagery or by inferring from indirect measurements (Cabral et al. 1990; Garrote 1992).

3. Case study

a. *The Sieve catchment*

The Sieve catchment, located in the Tuscany region, Italy, is used as a case study. The basin is bordered to the northeast by the Appennine Mountains, with a point of maximum elevation at Falterona Mountain (1657 m above mean sea level, MSL); to the north and west it is bordered by a series of mountain ranges of peak elevations of 800–900 m. The average elevation of the basin is 470 m MSL. The basin has moderate to high relief. The confluence of the Sieve with the main course of the Arno River is located 19 km upstream from the city of Florence. In 1971 the basin had 63 000 inhabitants.

For the use of rainfall information acquired through radar reflectivity, the catchment being studied must be divided into square surface areas, or pixels. All information detected by a radar system over a specific pixel is then summed, averaged, and converted in real-time into surface rainfall intensity by using an appropriate Z–R relationship.

Figure 2 shows a discrete, digitized representation of the Sieve Basin, in which every pixel is a square whose side is 400 m long. The catchment area is 840 km^2, represented by 5252 pixels, 1084 of which are "stream pixels," pixels saturated at all times and that serve as streamflow routing elements.

Figure 3 illustrates how the number of each pixel type varies with time as the basin is wetted by constant intensity (5 mm h^{-1}), 36-h duration storm, starting from a fairly dry initial state. There are four possible pixel types (or states) at any time.

(i) *Stream pixels:* these pixels represent "rivers," and therefore are assumed to be completely saturated at all times.

(ii) *Water table at the surface:* pixels where the water table is very shallow, normally occurring in concave regions of hillslopes near channels. Both pixel types (i) and (ii) have a runoff coefficient of 1 (i.e., infiltration capacity is 0) and also may generate return flow.

(iii) *Unsaturated (or Hortonian) pixels:* in these pixels the surface is not saturated, and they generate

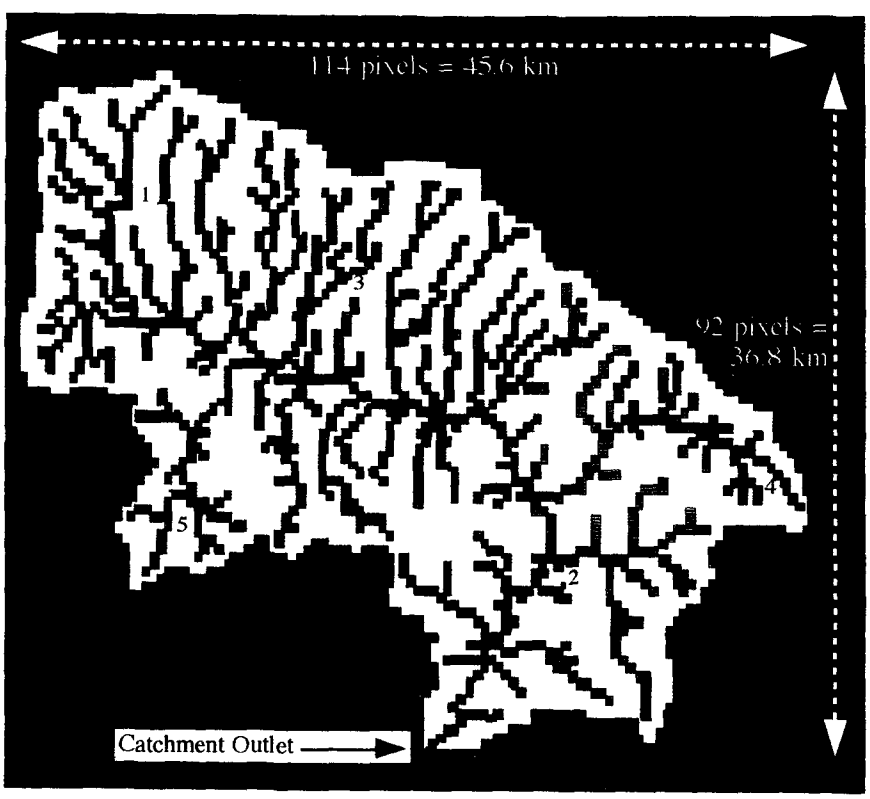

FIG. 2. A digitized discrete representation of the Sieve catchment. The picture elements (pixels) are squares of 400-m side. Numbers 1–5 represent the locations of arbitrarily selected pixels used in the storm distribution analysis.

Unauthenticated | Downloaded 04/18/24 09:57 AM UTC

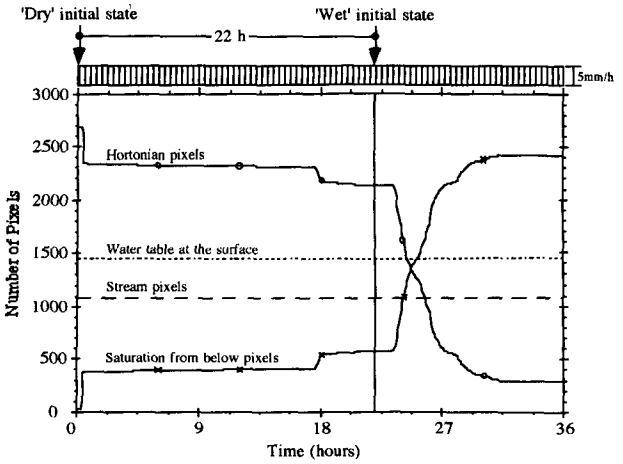

FIG. 3. The pixel-type evolution in time resultant from the simulation of a 36-h duration 5 mm h^{-1} uniform rainfall event.

only runoff through a Hortonian mechanism, that is, when the rainfall intensity is greater than the hydraulic conductivity.

(iv) *Saturated from below pixels:* in these pixels, the top front is at the surface. They can generate infiltration excess runoff (but with a different infiltration capacity than that of the unsaturated pixels) or return flow. The four types of pixels should add up to the total number of pixels in the basin at any time.

The analyses carried out in this study start with the river basin in a "wet" initial state. This "wet" state is defined in Fig. 3 and is reached after 22 h of simulation of 5 mm h^{-1} uniform rainfall. By starting our experiments with this "wet" initial condition, we are driving the basin at its most sensitive state. It is shortly after this condition that the nature of runoff production changes rapidly. The whole model and basin are very dynamic and are "used" to their full extent at this point. Dryer states will be far more insensitive to the nature of the input.

b. *The weather radar rainfall data*

The rainfall data used in this study are derived from two weather radars, MIT S-band and MIT C-band.

TABLE 1. Characteristics of the MIT S-band radar.

Parameter	Value
Wavelength	11.1 cm
Beamwidth	1.45°
Pulse length	1 μs (150-m resolution)
Sampling ($r > 50$ km)	1° × 1 km
Recorded precision	0.5 dBZ
Range	200 km

TABLE 2. Characteristics of the MIT C-band radar.

Parameter	Value
Wavelength	5.3 cm
Beamwidth	1.65°
Pulse length	0.5, 1.9 μs
Sampling (variable assignment in range)	224 range gates
Recorded precision	≤ 0.5 dBZ
Range	113 km

The MIT S-band weather radar station is located at MIT in Cambridge, Massachusetts (42.4°N, 71.1°W). Some of the station's characteristics are shown in Table 1. Table 2 gives the characteristics of the MIT C-band weather radar station, which was used to collect data near Darwin, Australia (12.5°S, 131.3°E).

Five storm events are used in the sensitivity experiment. They are described in Table 3. The storm events are represented by a series of matrices (i.e., radar frames), which are available in 5-min time intervals. Each matrix element corresponds to the rainfall intensity relative to a 400-m × 400-m pixel. The arithmetic mean, the standard deviation, and the maximum value of all the matrix elements (rainfall intensities) for each and every radar frame are plotted in Figs. 4–8 for the five rainfall events. The minimum rainfall intensity values have not been indicated in Figs. 4–8 since the storm areas were all smaller than the river basin area, and in all the events there were always one or more radar pixels indicating "zero" rainfall. Note that the values shown are not point estimates but averages over 400-m × 400-m pixels, and hence, maximum intensity may be smaller than corresponding point values. It is also important to keep in mind that partial coverage by the storm is a condition that argues strongly for the use of radar.

4. The sensitivity analyses

a. *The influence of radar data time resolution on the hydrograph*

Hudlow et al. (1981) have discussed the hydrological requirements for precipitation measurements, and

TABLE 3. A classification of the five rainfall events used in the sensitivity investigation.

Event	Type	Season of the year	Number of radar frames	Radar station
1	Convective	Summer 1990	33	C band
2	Convective	Summer 1990	42	C band
3	Stratiform	Spring 1991	78	S band
4	Stratiform	Spring 1988	90	S band
5	Convective	Summer 1989	21	C band

Unauthenticated | Downloaded 04/18/24 09:57 AM UTC

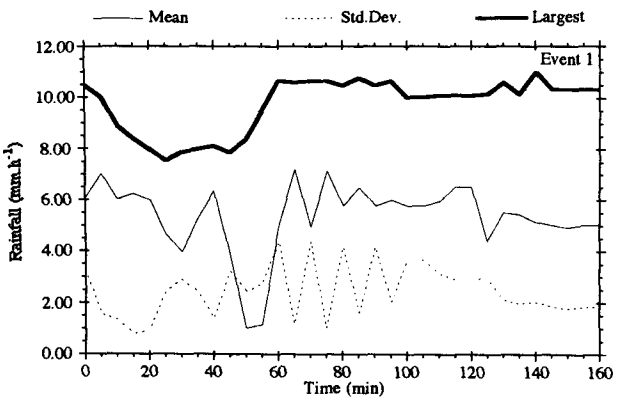

FIG. 4. Rainfall event 1. Shown are the spatial average, the largest value at any time, and the standard deviation around the spatial average.

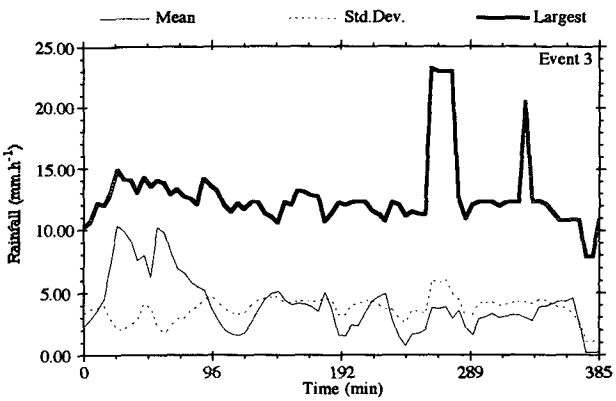

FIG. 6. Rainfall event 3. Shown are the spatial average, the largest value at any time, and the standard deviation around the spatial average.

pointed out that the uncertainty in the measurements depends, among other aspects, upon the temporal averaging needed for a particular hydrological requirement. According to Barrett and Monro (1981) and Niemczynowicz and Jonsson (1981), "the shorter the integration period, the larger is the maximum acceptable error."

In this section, the influence of the time integration of the rainfall amounts on the hydrographs is analyzed by the integration of the radar rainfall data in time and comparison of the generated hydrographs. All data was collected at 5-min intervals and then aggregated and averaged over longer intervals to carry out this experiment. Figures 9–13 show the comparisons among 5-, 15-, and 30-min radar-data-derived hydrographs for the five storm events. The time integration has no significant effect on the hydrological response, and both the 15- and 30-min rainfall data could therefore be used with virtually no loss in hydrograph accuracy. However, for convective rainfall even more intense than the data used in this study, there may be more sensitivity to the degradation of temporal resolution.

b. The influence of radar data spatial resolution on the hydrograph

Beven and Hornberger (1982) and Hamlin (1983) have stated that the accurate portrayal of the spatial variation in rainfall is a prerequisite for accurate simulation of streamflow. In addition, based upon a number of experiments with a hydrological model, Wilson et al. (1979) reported that it was clear that the spatial distribution of rainfall has a marked influence upon the behavior of the hydrograph. It was found that, even in cases where the total depth of precipitation is correctly estimated by an existing raingage network and even when the temporal character of the precipitation is accurately recorded, there could be serious errors in

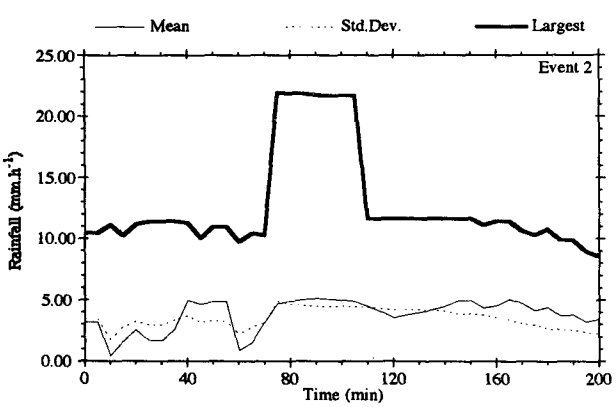

FIG. 5. Rainfall event 2. Shown are the spatial average, the largest value at any time, and the standard deviation around the spatial average.

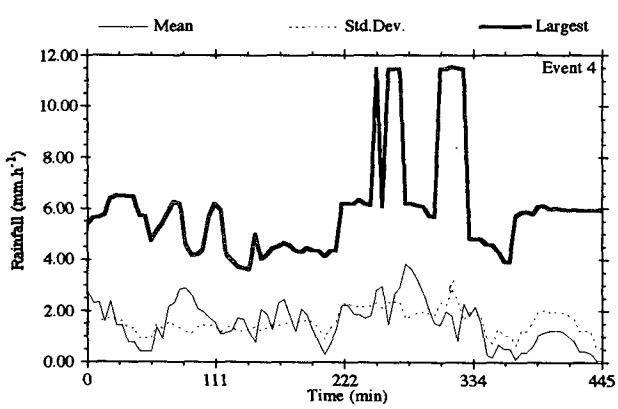

FIG. 7. Rainfall event 4. Shown are the spatial average, the largest value at any time, and the standard deviation around the spatial average.

Unauthenticated | Downloaded 04/18/24 09:57 AM UTC

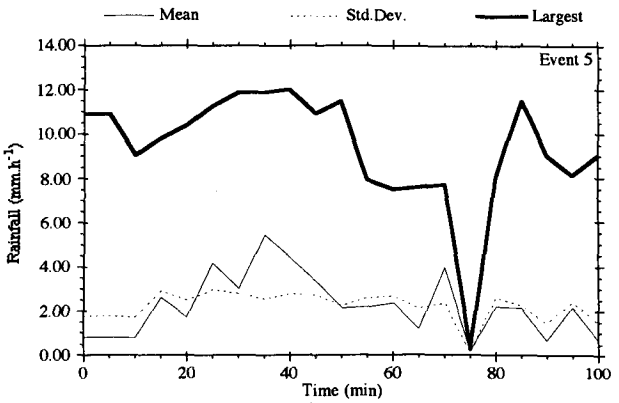

FIG. 8. Rainfall event 5. Shown are the spatial average, the largest value at any time, and the standard deviation around the spatial average.

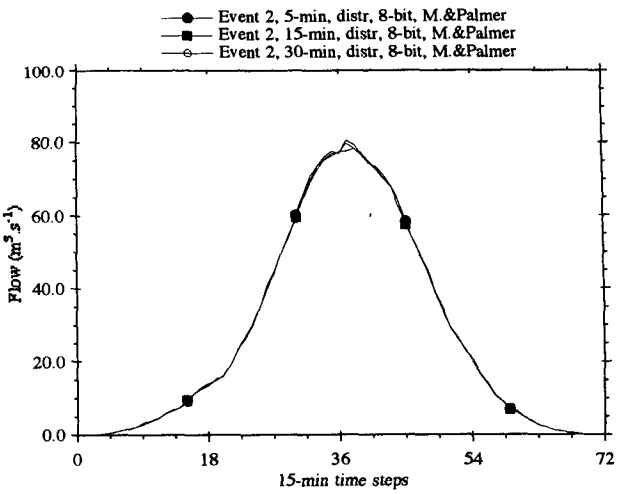

FIG. 10. The time integration analysis for event 2. Hydrographs corresponding to 5-, 15-, and 30-min rainfall temporal averages are shown.

the total volume, the peak, and the time-to-peak of the estimated hydrograph when the spatial pattern of precipitation was not properly represented in the input data. Such errors could be large in frontal rainfall, but were found to be even greater for intense, localized, convective storms.

In order to investigate the influence of the spatial variability of rainfall events on the modeled hydrographs, distributed radar-rainfall-derived hydrographs are compared to lumped radar-rainfall-derived hydrographs (Figs. 14–18) for the five storm events. Additionally, the effect of representing the precipitation for the whole catchment area by averaging the radar rainfall series of a few pixels, which are sparsely distributed over the catchment area, is investigated. To do so, five pixels were arbitrarily (i.e., randomly) selected within the Sieve catchment area and numbered from 1 to 5 (see Fig. 2). Figures 14–18 show the effect of representing events 1–5, respectively, in terms of the rainfall series observed at pixel 1 only. The figures also show the effect of representing the precipitation for the whole catchment area using the arithmetic mean of pixels 1 and 2; pixels 1, 2, and 3; pixels 1, 2, 3, and 4; and finally pixels 1, 2, 3, 4, and 5.

Even for the least spatially variable stratiform events 3 and 4 (Figs. 16 and 17), the use of a couple of radar pixels to represent the rainfall for the whole catchment area can lead to significant errors. It can also be observed from the figures that even the use of the five

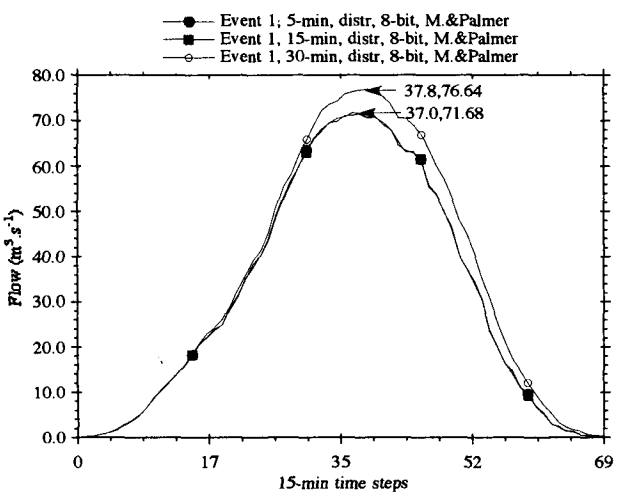

FIG. 9. The time integration analysis for event 1. Hydrographs corresponding to 5-, 15-, and 30-min rainfall temporal averages are shown.

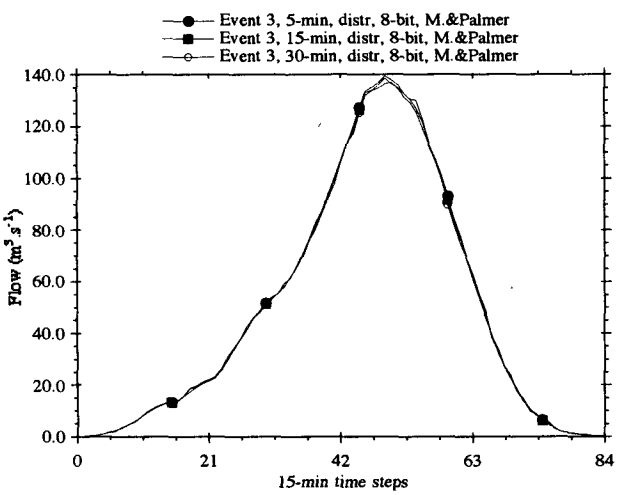

FIG. 11. The time integration analysis for event 3. Hydrographs corresponding to 5-, 15-, and 30-min rainfall temporal averages are shown.

Unauthenticated | Downloaded 04/18/24 09:57 AM UTC

sparsely located pixels (i.e., 1 gauge per 168-km^2 density) can produce hydrographs that are considerably different (both in timing and magnitude) from the fully distributed radar data. These results are totally in agreement with the findings of Wilson et al. (1979). However, the hydrographs obtained from the fully distributed and from the integrated (lumped) radar image are not so different from one another. For the storms studied, appropriately spatially averaged rainfall data (at 5-min time resolution and 8-bit accuracy) seem sufficient for use in the Sieve River basin.

c. *The influence of signal quantization on the hydrograph*

Signal quantization (Tilford 1987) refers to the number of discrete numerical levels that will represent the observed rainfall. Since most present-day digitizers produce binary outputs compatible with digital computers, it is convenient to adopt binary notation and describe the number of levels by the number of bits produced. Typical ranges used in electronic devices are of 3–16 bits, which correspond to a number of levels of 8–65 536 (2^3–2^{16} levels). The highest resolution of estimates of rainfall derived from weather radar is usually 8-bit precision.

Tilford (1987) has analyzed the use of low radar signal quantization using a transfer-function flood-forecasting model, and Cluckie et al. (1991) have done a similar analysis using a flood simulation model for urban drainage systems. In both investigations the conclusion is that low-resolution data are adequate for flood forecasting and simulation when those particular models are used. The effect of radar signal quantization upon the simulation of flows is investigated in this sec-

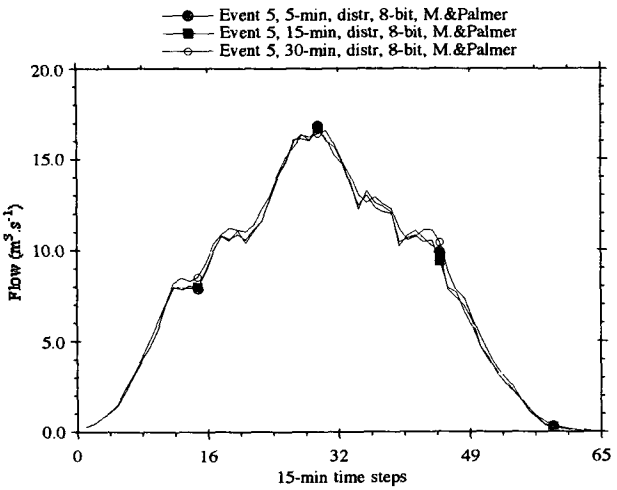

FIG. 13. The time integration analysis for event 5. Hydrographs corresponding to 5-, 15-, and 30-min rainfall temporal averages are shown.

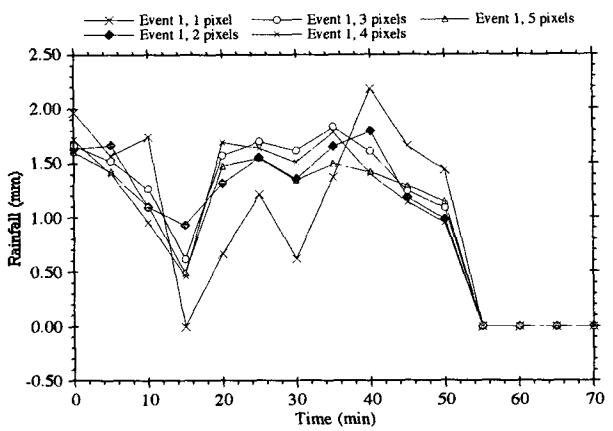

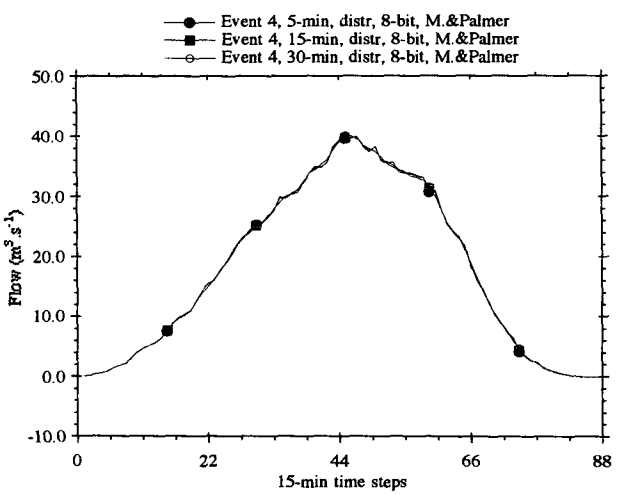

FIG. 12. The time integration analysis for event 4. Hydrographs corresponding to 5-, 15-, and 30-min rainfall temporal averages are shown.

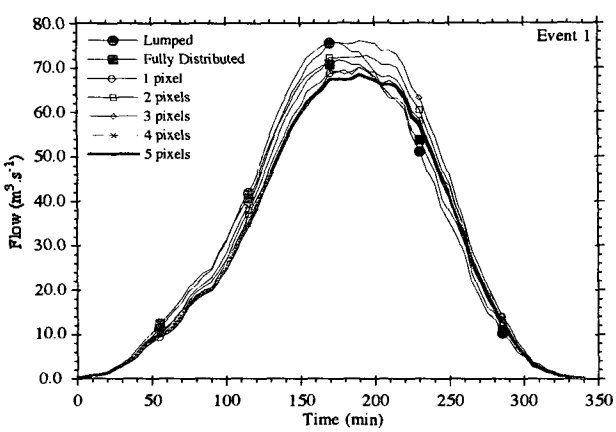

FIG. 14. The spatial distribution analysis for event 1. Top: rainfall (mm); bottom: flow (m^3 s^{-1}). Rainfall and discharges corresponding to spatially averaged radar inputs, fully distributed radar inputs, and rainfall from one, two, three, four, and five pixels are shown.

Unauthenticated | Downloaded 04/18/24 09:57 AM UTC

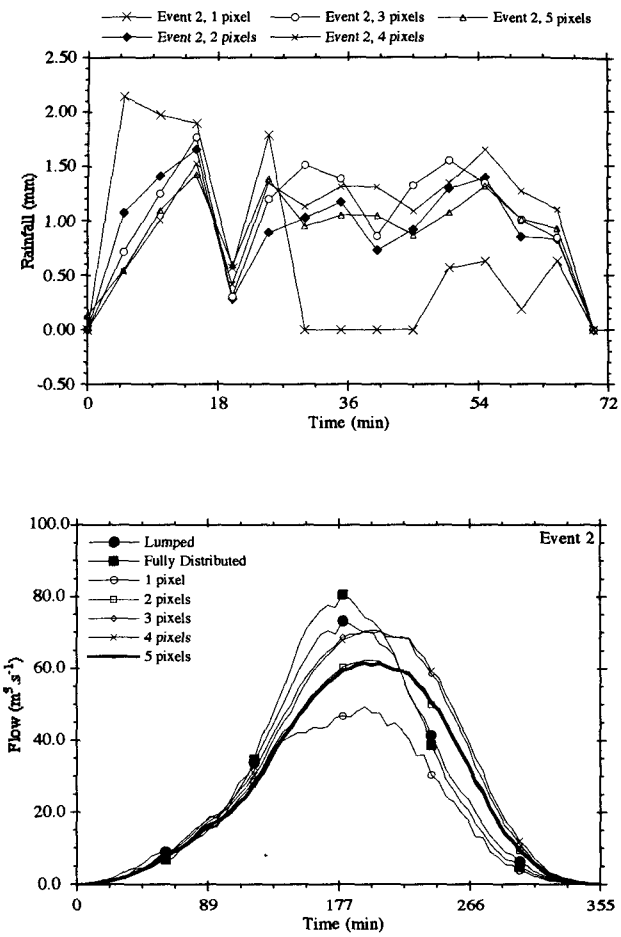

FIG. 15. The spatial distribution analysis for event 2. Top: rainfall (mm); bottom: flow ($m^3 s^{-1}$). Rainfall and discharges corresponding to spatially averaged radar inputs, fully distributed radar inputs, and rainfall from one, two, three, four, and five pixels are shown.

tion by comparison of hydrographs using 8-bit and 3-bit rainfall data as input to the DBS rainfall–runoff model.

Figures 19–23 show the comparisons between 3-bit and 8-bit radar-data-derived hydrographs for the five storm events using a 5-min time resolution and the distributed 400-m spatial resolution. As it may be observed from the figures, the differences in the peak flows were not very large (<20%), and timing differences were not observed. As a consequence, it may be concluded that 3-bit radar data could well be used in hydrological applications with reasonable compromise in accuracy, which is in agreement with the findings of Tilford (1987), at least for stratiform and moderately strong convective rainfall.

d. The influence of the Z–R relationship on the hydrograph

A great variety of Z–R relationships are found in the current literature (for a review, see Battan 1973). The one most universally used, and which is known as the standard Z–R relationship, was presented by Marshall and Palmer (1948) for stratiform rainfall:

$$Z = 200R^{1.6}. \quad (1)$$

Austin (1987) discussed physical factors that affect the relation between radar and raingage measurements of rain, using the MIT weather radar and New England storms, and has suggested the use of the relation

$$Z = 230R^{1.4}, \quad (2)$$

in preference to the traditional Marshall and Palmer equation (for stratiform rainfall) and the use of the relation

$$Z = 230R^{1.2} \quad (3)$$

for some types of convective storms.

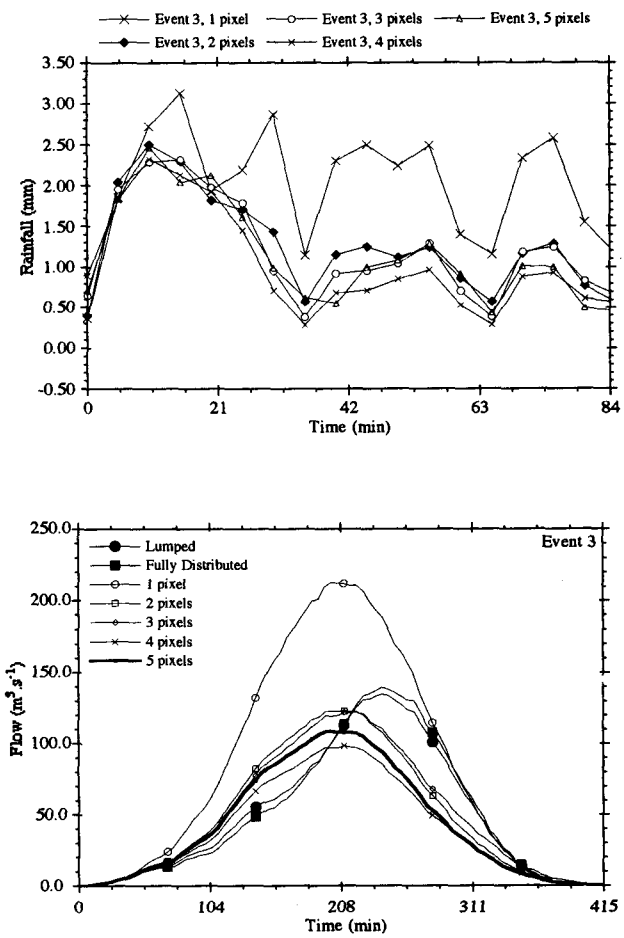

FIG. 16. The spatial distribution analysis for event 3. Top: rainfall (mm); bottom: flow ($m^3 s^{-1}$). Rainfall and discharges corresponding to spatially averaged radar inputs, fully distributed radar inputs, and rainfall from one, two, three, four, and five pixels are shown.

Unauthenticated | Downloaded 04/18/24 09:57 AM UTC

In this section, hydrographs derived by the DBS rainfall–runoff model using radar rainfall estimates based on the Z–R relations of Marshall and Palmer [Eq. (1)] and Austin [Eqs. (2) and (3)] are compared. For this analysis, Eqs. (1) and (2) were used for the stratiform events (Figs. 26 and 27), and Eqs. (1) and (3) for the convective events (Figs. 24, 25, and 28). It may be observed from the figures that the use of an appropriate Z–R relationship can significantly affect the hydrological response. It can also be observed that depending on the Z–R equation that is used, the differences in peak can be significant, particularly in the convective cases. These results lead to the conclusion that for hydrological applications using radar data, it is important to identify the storm type for the use of a proper Z–R equation. For the particular case of flood forecasting, the use of techniques for automatic storm-type recognition would probably be helpful.

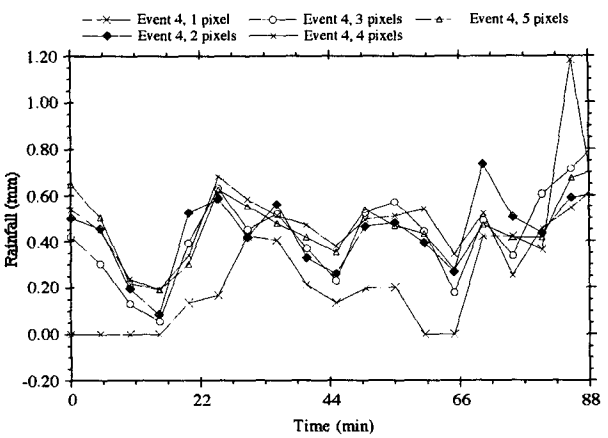

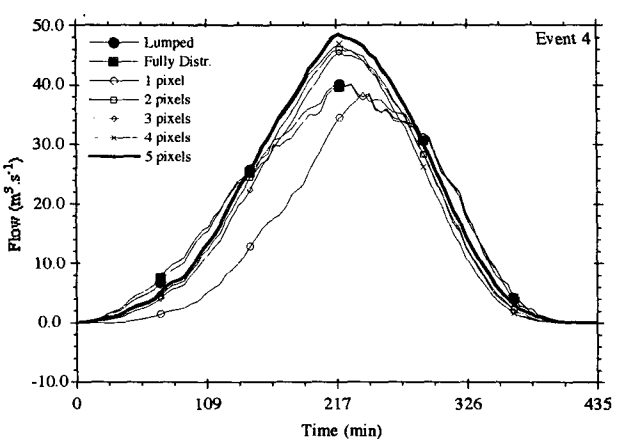

FIG. 17. The spatial distribution analysis for event 4. Top: rainfall (mm); bottom: flow ($m^3 s^{-1}$). Rainfall and discharges corresponding to spatially averaged radar inputs, fully distributed radar inputs, and rainfall from one, two, three, four, and five pixels are shown.

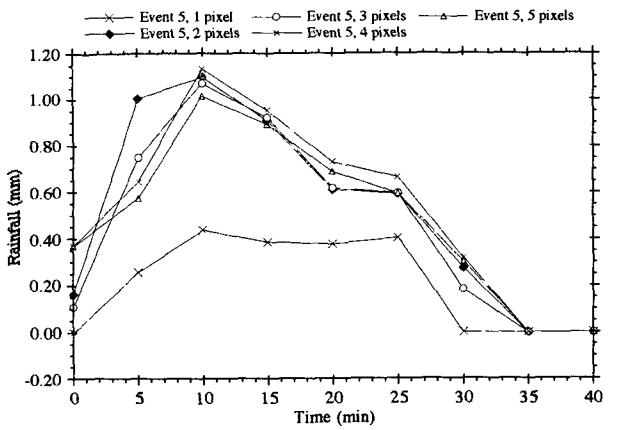

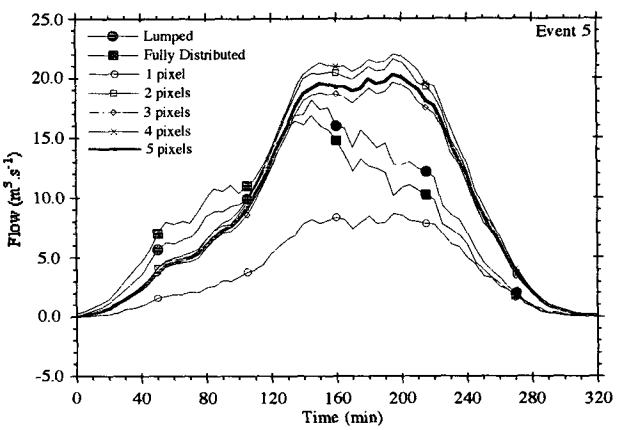

FIG. 18. The spatial distribution analysis for event 5. Top: rainfall (mm); bottom: flow ($m^3 s^{-1}$). Rainfall and discharges corresponding to spatially averaged radar inputs, fully distributed radar inputs, and rainfall from one, two, three, four, and five pixels are shown.

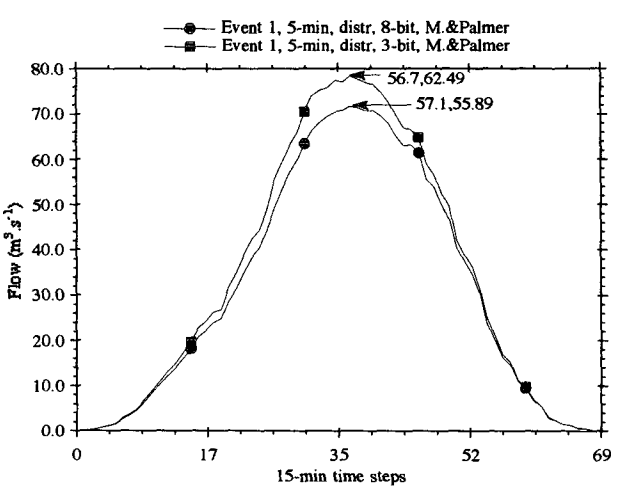

FIG. 19. The radar quantization analysis for event 1. Discharges resulting from 3- and 8-bit numerical representation of radar rainfall.

Unauthenticated | Downloaded 04/18/24 09:57 AM UTC

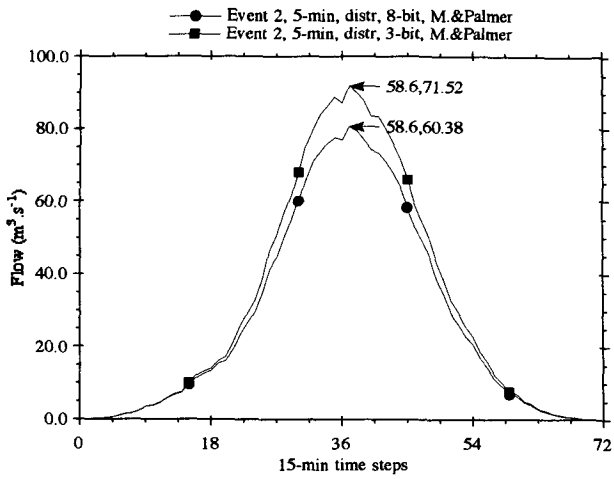

FIG. 20. The radar quantization analysis for event 2. Discharges resulting from 3- and 8-bit numerical representation of radar rainfall.

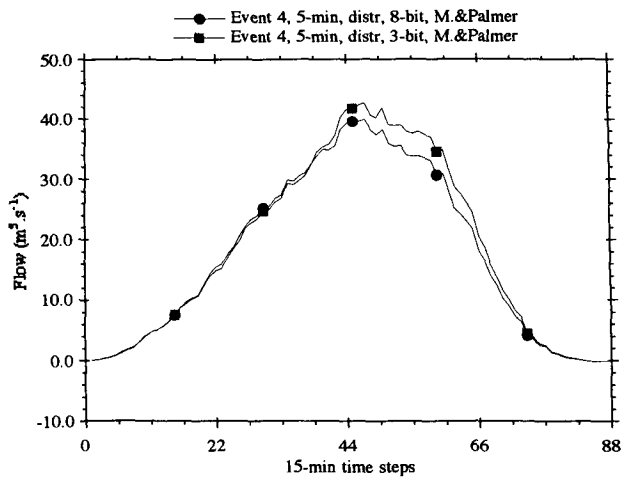

FIG. 22. The radar quantization analysis for event 4. Discharges resulting from 3- and 8-bit numerical representation of radar rainfall.

5. Conclusions

Hydrologists have generally relied on point (raingage) measurements of precipitation, under the crude assumption that such data can represent area rainfall for all purposes and event types. However, as it is shown in this paper, rainfall events can be very variable in both time and space. It is recognized that spatial variability of the hydrological phenomena can be more realistically simulated through the use of weather radar that provides distributed rainfall amounts at acceptable levels of accuracy. It is certain that even if radar could not improve upon the absolute magnitude of the rainfall amount, it would still provide most valuable information upon the spatial variation and evolution of the precipitation events.

It is worth mentioning that even if there were no actual errors in either gauge or radar measurements, there might be significant discrepancies between measured amounts of rainfall at any location site because of differences in sampling modes. The radar samples, almost instantaneously, a volume of atmosphere that may have a surface projection of several square kilometers, and measurements are repeated at intervals of several minutes. The gauge continuously accumulates rain falling on an area that is generally much smaller than a square meter. At any instant, rainfall intensity often varies significantly over distances of less than a kilometer, while at any point it may change during time intervals of a minute or less. Therefore, the rain sampled by the gauge may not be representative of that in the entire area beneath the radar-sampled volume.

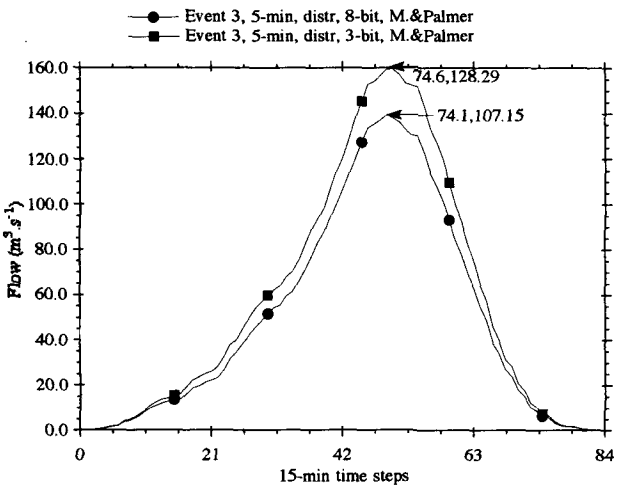

FIG. 21. The radar quantization analysis for event 3. Discharges resulting from 3- and 8-bit numerical representation of radar rainfall.

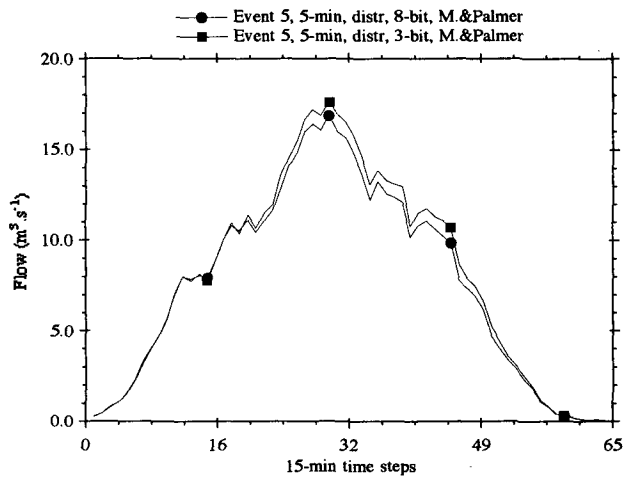

FIG. 23. The radar quantization analysis for event 5. Discharges resulting from 3- and 8-bit numerical representation of radar rainfall.

Unauthenticated | Downloaded 04/18/24 09:57 AM UTC

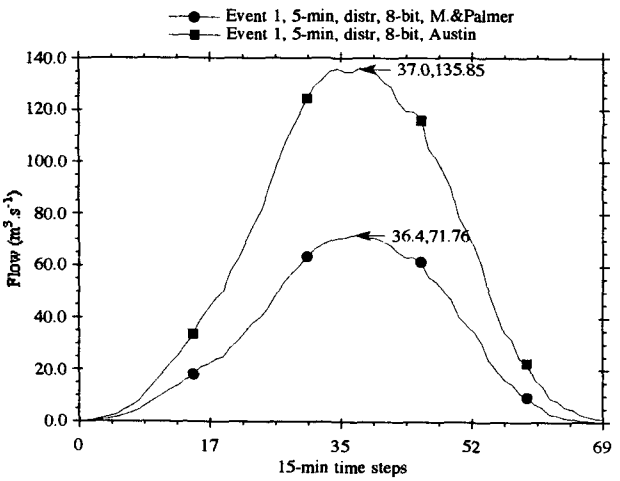

FIG. 24. The Z–R relationship analysis for event 1. Discharges resulting from 8-bit numerical representation of radar rainfall.

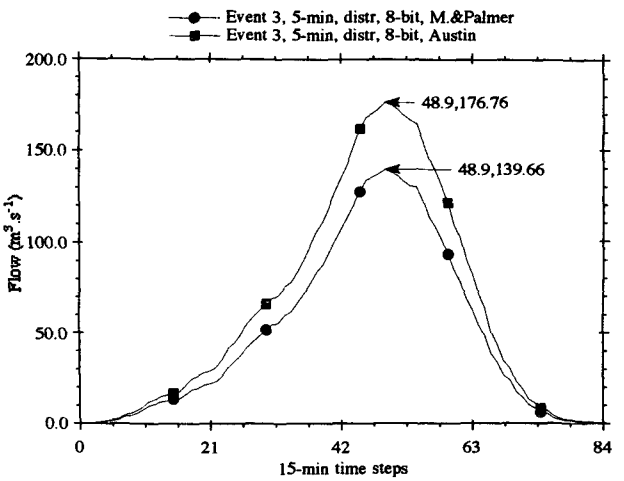

FIG. 26. The Z–R relationship analysis for event 3. Discharges resulting from 8-bit numerical representation of radar rainfall.

In a flood warning context, it is of fundamental importance for the decision makers to be aware of the rainfall–runoff capabilities of meteorological radar, as well as of its limitations and uncertainties. In addition, during a flood event, it is important to bear in mind that electronic systems, schemes, and equipment may fail. If, for instance, the weather radar station becomes inoperative, it is invaluable to know how the rainfall–runoff model and the particular catchment would behave if raingages became the only source of rainfall information. Figures 14–18 show the rainfall series obtained by using one, two, three, four, and five radar pixels to represent the rainfall intensities over the catchment area. As it may be observed from the figures, the storm events proved to be, in some occasions, considerably variable in space, and the use of rainfall data obtained from the records of a single pixel to represent the precipitation over the whole area might not realistically represent the phenomenon.

The time-resolution investigation carried out in this study showed no significant difference between hydrographs generated from 5-, 15-, and 30-min radar rainfall data. It is worth mentioning that 30-min time resolution may be inappropriate for stronger convective events and/or catchment basins with faster hydrologic response times.

From the comparisons between hydrographs generated by 3-bit and 8-bit radar data, it is possible to infer that 3-bit data could well be used to simulate the events used in this investigation since the differences

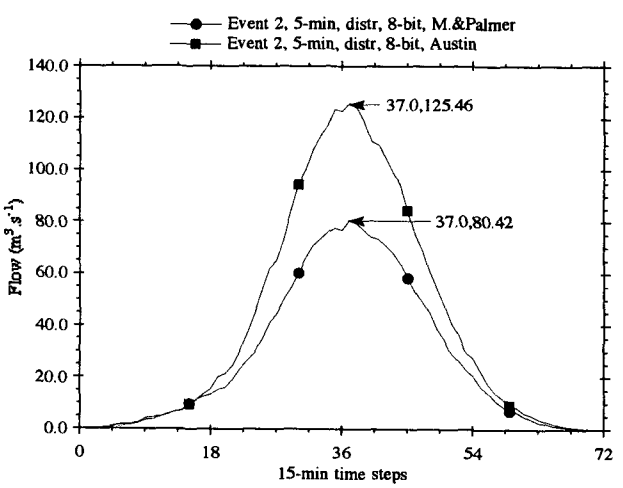

FIG. 25. The Z–R relationship analysis for event 2. Discharges resulting from 8-bit numerical representation of radar rainfall.

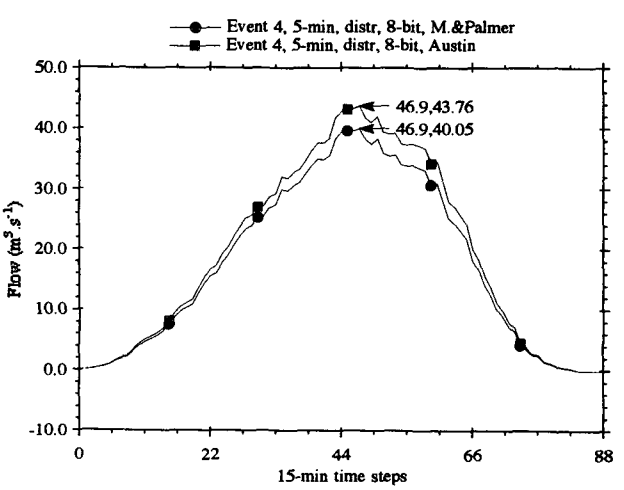

FIG. 27. The Z–R relationship analysis for event 4. Discharges resulting from 8-bit numerical representation of radar rainfall.

Unauthenticated | Downloaded 04/18/24 09:57 AM UTC

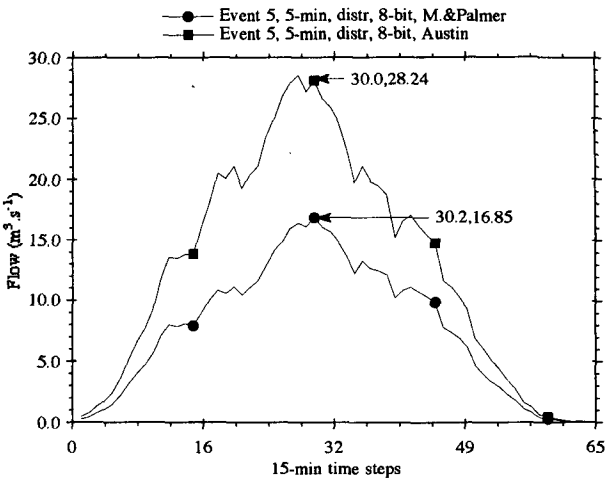

FIG. 28. The Z–R relationship analysis for event 5. Discharges resulting from 8-bit numerical representation of radar rainfall.

in peak flow and time-to-peak were unimportant. This would certainly be of some benefit in terms of saving time and computer storage, and it would also speed up communication and therefore benefit flood-warning schemes, especially for urban fast-response basins.

The use of radar for quantitative precipitation measurements is a relatively recent technique. There is still a great deal to be done, and radar has been definitely opening the way for further research in both hydrology and meteorology. Already, some improvement in radar distributed rainfall estimates has been realized by selecting Z–R relationships based upon storm type. The progress, however, has been slow because of large variations within storm-type classification. The hydrographs produced in this investigation by the DBS rainfall–runoff model using radar precipitation data obtained from Marshall and Palmer and the two Austin Z–R relationships showed that they may differ from one another (see, for instance, the 89% difference in peak magnitude for event 1 and the 56% for event 2). As a consequence, it is recommended that methods be developed for the automatic recognition of the storm types in real time. These methods would allow the selection of the appropriate Z–R relationship to be used with any particular storm type.

The investigation presented in this paper indicates, that for the stratiform and moderately strong convective events analyzed, using degraded resolution for one of the data characteristics (spatial, temporal, or quantitative) can be as useful in hydrologic modeling as the full resolution. Thus, using a lumped rather than the distributed spatial resolution, or using 3-bit rather than 8-bit data precision, or using 15- and 30-min rather than 5-min data can still provide useful hydrologic information. Further investigation is recommended to verify whether or not this conclusion holds for rainfall events other than the five analyzed in this paper, especially for those associated with very intense rainfall, for catchment areas different from the Sieve's 840 km^2, and for different hydrological models. If so, a significant reduction in data processing, transmission, and storage can be achieved. Consequently, real-time flood forecasting using radar data could be performed not only faster but also less expensively.

Acknowledgments. The authors would like to thank CAPES, the Brazilian Government body who has financially supported the first author. We also acknowledge the support of the U.S. National Weather Service (Cooperative Agreement NA90AA-H-HY530), the Army Research Office (Contract DAAL0-89-K-0151), the National Research Council of Italy through a Cooperative Agreement with the University of Florence, and the National Science Foundation (Cooperative Agreement CES-8815725). Thanks also to Dr. L. M. Garrote, for the discussion of the DBS model. The opinions presented here are those of the authors and not the position of the sponsors.

REFERENCES

Austin, P. M., 1987: Relation between measured radar reflectivity and surface rainfall. *Mon. Wea. Rev.*, **115,** 1053–1071.

Barrett, C. B., and J. C. Monro, 1981: National prototype flash flood warning system. Preprint, *Fourth Conf. on Hydrometeorology,* Reno, 234–239.

Battan, L. J., 1973: *Radar Observation of the Atmosphere.* The University of Chicago Press, 324 pp.

Becchi, I., E. Caporali, G. Federici, and E. Palmisano, 1989: Un modello distribuito per lo studio del bacino dell'Arno: Analisi idrologica della Sieve. (A distributed model for the study of the Arno river basin: A hydrological analysis of the Sieve). *Acqua Aria,* **10–89,** 1129–1144.

Beven, K. J., and G. M. Hornberger, 1982: Assessing the effect of spatial pattern of precipitation in modeling stream flow hydrographs. *Water Resour. Bull.,* **18,** 823–829.

Brooks, R. H., and A. T. Corey, 1964: Hydraulic properties of porous media. Hydrology Paper 3. Colorado State University, Fort Collins, CO, 30 pp.

Browning, K. A., and C. G. Collier, 1969: Nowcasting of precipitation systems. *Rev. Geophys.,* **27,** 345–370.

Cabral, M. C., R. L. Bras, D. Tarboton, and D. Entekhabi, 1990: A distributed, physically based rainfall-runoff model incorporating topography for real-time flood forecasting. Ralph M. Parsons Laboratory, Report No. 332, Massachusetts Institute of Technology, Cambridge, MA, 220 pp.

Cluckie, I. D., K. A. Tilford, and G. W. Shepherd, 1991: Radar signal quantization and its influence on rainfall-runoff models. *Hydrological Applications of Weather Radar. Proc. of the Int. Symp. on Hydrological Applications of Weather Radar,* Salford, UK, Ellis Horwood, 440–451.

Collier, C. G., 1989: Applications of weather radar systems. A guide to uses of radar data in meteorology and hydrology. *Series in Space Science and Space Technology,* E. Horwood, Ed., Halstead, 294 pp.

Garrote, L., 1992: Real-time modeling of river basin response using radar-generated rainfall maps and a distributed hydrologic database. Engineers degree thesis. Department of Civil and Environmental Engineering, Massachusetts Institute of Technology, 501 pp.

Unauthenticated | Downloaded 04/18/24 09:57 AM UTC

Georgakakos, K. P., 1986: Generalized stochastic hydrometeorological model for flood and flashflood forecasting. 1: Formulation. *Water Resour. Res.*, **22,** 2083–2095.

Georgakakos, K. P., and M. L. Kavvas, 1987: Precipitation analysis, modeling, and prediction in hydrology. *Rev. Geophys.*, **25,** 163–178.

——, and G. F. Smith, 1990: On improved hydrologic forecasting: Results from a WMO real-time forecasting experiment. *J. Hydrol.*, **114,** 17–45.

Goodrich, D. C., and D. A. Woolhiser, 1991: Catchment hydrology. *Rev. Geophys.*, **29,** 202–209.

Hamlin, M. J., and D. H. Rees, 1987: The use of rainfall forecasts in the optimal management of small-holder rice irrigation: A case study. *Hydrol. Sci. J.*, **32,** 15–29.

Hudlow, M., 1988: Technological developments in real-time operational hydrologic forecasting in the United States. *J. Hydrol.*, **102,** 69–92.

Hudlow, M. D., R. K. Farnsworth, and D. R. Green, 1981: Hydrologic forecasting requirements for precipitation data from space measurements. *Precipitation Measurement from Space,* D. Atlas and O. W. Thiele, Eds., Goddard Space Flight Center, NASA, D23–D30.

Krajewski, W. F., 1987: Radar rainfall data quality control by the influence function method. *Water Resour. Res.*, **23,** 837–844.

Marshall, J. S., and W. M. Palmer, 1948: The distribution of raindrops with size. *J. Meteor.*, **5,** 165–166.

Niemczynowicz, J., and O. Jonsson, 1981: Extreme rainfall events in Lund. 1979–1980. *Nord. Hydrol.*, **12,** 129–142.

Smith, J. A., and W. F. Krajewski, 1987: Statistical modeling of space-time rainfall using radar and rain gage observations. *Water Resour. Res.*, **23,** 1893–1900.

Tarboton, D. G., R. L. Bras, and I. Rodriguez-Iturbe, 1989: Scaling and Elevation in River Networks. *Water Resour. Res.*, **25,** 2037–2051.

Tilford, K. A., 1987: Real-time flood forecasting using low intensity resolution radar rainfall data. M.Sc. thesis, Department of Civil Engineering, University of Birmingham, England, 67 pp.

Wilson, C. B., J. B. Valdes, and I. Rodriguez-Iturbe, 1979: On the influence of the spatial distribution of rainfall on storm runoff. *Water Resour. Res.*, **15,** 321–328.

Unauthenticated | Downloaded 04/18/24 09:57 AM UTC